EARTH OBSERVATION AND GEOMATICS ENGINEERING
website: https://eoge.ut.ac.ir

Fault distance-based approach in thermal anomaly detection before strong Earthquakes

Arash Karimi Zarchi[1*], Mohammad Reza Sarajian[1]

[1] Remote Sensing Department, School of Surveying and Geospatial Engineering, Collage of Engineering, University of Tehran, Tehran, Iran

Article history:
Received: 2023-02-18, Revised: 2023-06-18, Accepted: 2023-06-30

ABSTRACT

The recent scientific studies in the context of earthquake precursors reveal some processes connected to seismic activity including thermal anomaly before earthquakes which is a great help for making a better decision making regarding this disastrous phenomenon and reducing its casualty to a minimum. This paper presents a method for grouping the objective input data for different thermal anomaly detection methods using the land surface temperature (LST) mean in multiple distances from the corresponding fault during the 40 days (i.e. 30 days before and 10 days after the impending earthquake) of investigation. Six strong earthquakes with Ms > 6 that have occurred in Iran have been investigated in this study. We used two different approaches for detecting thermal anomalies: the mean-standard deviation method and the interquartile method. Results show that the proposed input data produces fewer false alarms in each of the thermal anomaly detection methods compared to the ordinary input data making this method much more accurate and stable regarding the easy accessibility of thermal data and their less complicated algorithms for processing. In the final step, the detected anomalies are used for estimating earthquake intensity using Artificial Neural Network (ANN). The results show that the estimated intensities of most earthquakes are very close to the actual intensities. Since the locations of the active faults are known a priori, using fault distance-based approach may be regarded as a superior method in predicting the impending earthquakes for vulnerable faults. In spite of the previous investigations that the studies were only possible aftermath, the fault distance-based approach can be used as a tool for future unknown earthquakes prediction. However, it is recommended to use thermal anomaly detection as an initial process to be jointly used with other precursors to reduce the number of investigations that require more complicated algorithms and data processing.

KEYWORDS

Earthquake Precursor
Thermal Anomaly
LST
Corresponding Fault
ANN

1. Introduction

Earthquake is one of the most difficult phenomena to predict and hence one of the most destructive natural calamities, capable of causing lots of instant loss of lives and property (Console, Pantosti, & D'Addezio, 2002). Earthquake is the result of surging tectonic stress and its release caused by tectonic movement in fault zones (Geller, Jackson, Kagan, & Mulargia, 1997). There have been a number of studies regarding the existing precursors for this natural disaster. These studies indicate some of the precursors such as water temperature, water level change, flow rate, magnetic field, electric field, soil/air temperature, relative humidity, ionospheres fluctuations, surface deformations, and land surface temperature (LST) anomalies (Cicerone, Ebel, & Britton, 2009; Hayakawa, Molchanov, Kodama, Tanaka, & Igarashi, 2000; Wyss, 1997; Yao, 2007).

Although each of these precursors has an important and individual role in estimating the earthquake parameters, the thermal anomaly precursor is one of the most useful ones due to its physical relevance to the nature of the earthquake. There are mainly five hypotheses describing the physical basis behind thermal anomaly related to seismic activities: 1) Earth degassing mechanism, 2) Groundwater anomaly, 3)

Frictional heating, 4) Seismo-ionosphere coupling, and 5) p-hole activation mechanism (Cicerone et al., 2009; Freund, 2011; Z. Qiang et al., 1999; Roeloffs, 1988). Each of these concepts will either directly increase the land surface temperature or they will increase the near-surface air temperature which would eventually cause a change in surface temperature depending on their effect (A. K. Saraf, Rawat, Choudhury, Dasgupta, & Das, 2009; Surkov, Pokhotelov, Parrot, & Hayakawa, 2006; Valerio Tramutoli, Di Bello, Pergola, & Piscitelli, 2001; Verma & Bansal, 2012).

The idea that thermal anomalies may be related to seismic activity was first put into application in the early eighties. In 1990, researchers detected thermal anomalies prior to an earthquake (Tronin, 1996). These researchers were among the first people who suggested using thermal infrared anomalies for a better understanding of the earthquake phenomena. Tramutoli (1998) used Robust AVHRR Approach (RAT) method for detecting thermal anomalies before the earthquakes using AVHRR data (Valerio Tramutoli, 1998). This method allowed Tramutoli to detect the thermal anomalies with better accuracy by separating the natural anomalies like the seasonal changes from the anomalies that were related to seismic activities (Valerio Tramutoli et al., 2001). Later this method was adjusted for the rest of the remote sensing data and it is now known as Robust Satellite Approach or RST (V Tramutoli, Cuomo, Filizzola, Pergola, & Pietrapertosa, 2005).

Originally, in order to describe the relationship between land surface temperature and seismic activities, AVHRR (Advanced Very High-Resolution Radiometer onboard NOAA satellite) data were used (Z.-j. Qiang, Xu, & Dian, 1997). Many studies such as Saraf (2009) and Choudhury (2006) several strong earthquakes using AVHRR data (Choudhury, Dasgupta, Saraf, & Panda, 2006; A. K. Saraf et al., 2009). In a few cases, they used the Defense Meteorological Satellite Program (DMSP) in certain situations like areas with snow or cloud cover in order to obtain higher accuracy (A. Saraf & Choudhury, 2005). Although they did not explore the statistical parameters of the anomaly and relied only on visual interpretation, their studies widened spatial coverage required to take an important step for future studies. Rawat in 2011, investigated Ms 5.9 Vrancea (Romania) earthquake on October 27th, 2004, and showed LST rise of 5–10 °C within a week of the earthquake (Rawat, Saraf, Das, Sharma, & Shujat, 2011).

In recent years, MODIS (Moderate Resolution Imaging Spectroradiometer) LST product has proven to be very useful as a direct input for several study cases and various anomaly detection methods. In 2004 Ouzounov and Freund were among the first researchers who used MODIS products as their input data for their studies (Ouzounov & Freund, 2004). They also investigated TIR anomalies and mid-IR emissions prior to an earthquake. Another study conducted one of the most destructive earthquakes that happened in Gujarat (India) on January 26th, 2001. The results showed an anomaly of 3–4 °C about 5 days before the earthquake (Ouzounov & Freund, 2004).

As mentioned, an earthquake occurs as a result of releasing the built-up stress along the fault. Therefore, active faults are one of the most important factors contributing to the earthquake process. Although many studies have focused on the subject of earthquakes, only a few have investigated the changes along the fault zones regarding their temperature. In 2010, Wang and Manga investigated the groundwater change in a fault zone that would later cause a change in land surface temperature in multiple earthquakes (Wang & Manga, 2021). Later in 2019, Li and Shi investigated anomalies in Earth degassing mechanism and groundwater in 2008 for Wenchuan Ms 8.0, 2013, Lushan Ms 7.0 and Kangding Ms 6.3, 2014 earthquakes near Xianshuihe fault zone (Li, Shi, Wang, & Liu, 2019). Although these studies were not directly about the thermal anomalies, the results showed releasing CO_2 and changes in the composition of groundwater that would later cause a change in land surface temperature. In 2020, Khalili et al. used yearly LST, air, and soil temperature of 5 years to investigate the thermal anomalies related to the Saravan earthquake (April 16th, 2013, Ms = 7.8). The results showed the thermal anomaly pattern before the Saravan earthquake. In the Kriging surfaces of the air temperature and the difference between the LST and air temperature, considerable changes were observed a few days before the earthquake and lasted a few days after it (Khalili, Abdollahi Eskandar, & Alavi Panah, 2020).

Recently, many studies use machine learning algorithms especially those involving Artificial Neural Network (ANN). ANN is a mathematical model and was adapted from human reactions and simulation of thinking processes to solve complicated problems. Using ANN, one can solve these problems without entering into complex theories and topics (Adeli, 1999). In 2014, Akhoondzadeh investigated Saravan earthquake in Iran that occurred on April 16th, 2013 using ANN with the help of Particle Swarm Optimization (PSO) to increase the efficiency of thermal anomaly detection (Akhoondzadeh, 2014). In 2020, Nekoee and Shah-Hosseini used two different methods of dynamic NARX (Nonlinear Auto Regressive with eXternal input) neural network algorithm namely Levenberg-Marquardt and Scaled conjugated gradient to investigate 3 earthquakes in Iran. NARX neural network was able to find anomalies of 5 to 7 degrees from 5 to 13 days prior to earthquake (Nekoee & Shah-Hosseini, 2020).

This paper presents a method of grouping input data to be

used in two different anomaly detection methods. Most of the studies on thermal anomalies are only possible after the earthquake happens since they require the location of the epicenter. The presented fault distance-based approach can be regarded as a better method for predicting the earthquake, as it uses a-priori known active faults. The conventional data selection methods use only LST and time, while the distance-based grouping of data proposed in this study would also take into the consideration one of the very influential parts of the earthquake effect which is the relevant fault and the regions around it. This study also intends to show the accuracy of using the combination of this assembled data and thermal anomaly detection results for estimating each earthquake's intensity using ANN.

2. STUDY AREAS AND DATASETS

2.1. Case Studies

Table 1. The earthquakes' locations, intensities and dates of six strong earthquakes (Ms>6) of Azgalah, Goharan, Saravan, Shonbeh, Brujerd, and Sari investigated in this study.

Table 1. The earthquakes' locations, intensities and dates.

Earthquake	Epicenter	Intensity	Date
Azgalah	34.81 N 45.83 E	7.3	November 12, 2017
Goharan	26.52 N 57.76 E	6.2	May 11, 2013
Saravan	27.11 N 62.05 E	7.8	April 16, 2013
Shonbeh	28.48 N 51.58 E	6.3	April 9, 2013
Brujerd	34.57 N 48.79 E	6.1	March 31, 2006
Sari	36.27 N 51.57 E	6.3	May 28, 2004

2.2. Datasets

In this study, MODIS sensor daily land surface temperature product (MOD11A1) during forty days (thirty days before and ten days after the earthquakes) for each earthquake has been used. The MODIS daily LST and emissivity data are retrieved at 1km pixel size by the generalized split-window algorithm, which uses bands 31 and 32.

In addition, the relevant active fault was identified and its shape file was extracted depending on how close it was to the location of each earthquake's epicenter.

3. METHODOLOGY

As mentioned, this paper presents a method of grouping input data for different thermal anomaly detection methods. It uses the land surface temperature mean in multiple distances of 1 to 20 km from the corresponding fault during the forty days starting from 30 days before and 10 days after a given earthquake event. To generate the input data and use it in the anomaly detection algorithm, the following steps have been performed: pre-processing, fault distant map generation, and land surface temperature diagram generation. The data are then used in anomaly detection methods and Artificial Neural Network (ANN).

3.1. Pre-processing

The first step is to remove the natural and observational noise signals, which are due to changes in seasons, view angles, and air density from the TIR data. By doing so, the remaining data would be mainly unmixed TIR anomaly data associated with increased seismic activity. In order to achieve this, a linear function was fitted to the LST of the previous year where there was no strong seismic activity and then was subtracted from the present year of LST in which the earthquake had occurred.

3.2. Fault distant map

In order to use the fault in our process, it is necessary to have an understanding of the corresponding fault and its surrounding areas in different distances. A fault distant map is a map that its pixels represent values depending on how far they are from the fault. The closer the pixel is to the fault, the lower its value and it will increase as we get further from it. Figure 1 shows the example of Azgalah fault distant map.

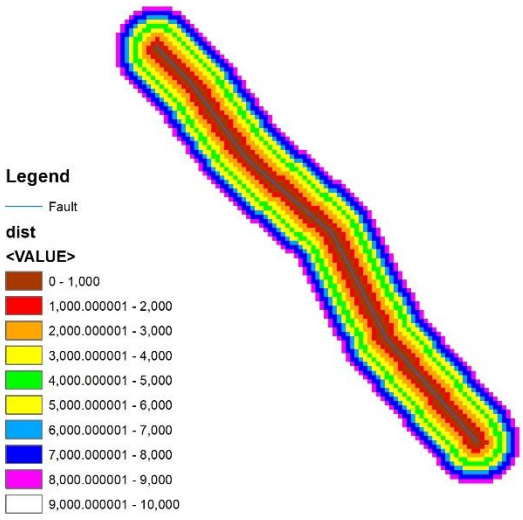

Figure 1: Fault distant map for Azgalah study case

3.3. Land surface temperature diagram

In this study, a method of using the temperature mean in different buffer zones with various radiuses (i.e. 1-20 km) around the corresponding active fault during the period of investigation has been presented. The data is presented by a 3D diagram, made by the LSTs mean in different radiuses around the corresponding active fault in each day. This means that each pixel in this data which can be represented as a picture or 3D diagram shows the LST mean in a certain radius buffer zone for a specific day. It should be noted that the width of each buffer is only 1 km and R is the buffer radius (distance) from the related fault. Later, these temperatures mean of each buffer is used as input data to test various anomaly detection methods such as the interquartile method and the standard deviation method.

Instead of using conventional 2D-data, the anomaly detection methods will act more appropriately by using the 3D-data which includes LST mean values in different buffers, time lapses (days) to the earthquake events, and the distances from the fault.

3.4. Anomaly detection methods

Two anomaly detection methods have been used. The first one is simply the use of mean and standard deviation (1) of LST values (Akhoondzadeh, 2011) in each buffer zone.

$$x > \mu + k \times \sigma \qquad (1)$$

Where μ is the mean value, σ is the standard deviation value of the LSTs and k is a coefficient around 1.6 but may slightly change for each case study. For each x (i.e. LST), if the result of (1) is true, it will be regarded as an anomaly.

The second anomaly detection method uses a similar approach but instead of using mean and standard deviation, it uses median and interquartile range (2) (Saradjian and Akhoondzadeh, 2011) which is known as the Interquartile method.

$$x > M + k \times IQR \qquad (2)$$

Where M is the median value, IQR is the interquartile range and k is a coefficient around 1.3 but may slightly change for each case study. Like the first method, if each x (i.e. LST) is greater than equation 2, then the behavior of the LST will be regarded as anomalous.

3.4. Artificial Neural Network (ANN)

ANN has shown to be one of the most reliable methods for solving complicated problems. Many studies have described its theoretical background (Cheng and Li, 2008; Chung, Lee, and Pearn, 2005; Ergu, Kou, Shi, and Shi, 2014; Sahoo, Dhar, and Kar, 2016). ANN is a mathematical network model trained by using a specific set of data. This trained network can later be used to transform other sets of data into output (Nedic, Despotovic, Cvetanovic, Despotovic, and Babic, 2014). Most ANNs consist of three different layers: the input layer, which is a layer for initiating data, the hidden layer, which could have multiple layers depending on the nature and complexity of the problem, and the output layer (Pradhan and Lee, 2009). Inside each layer lays a number of neurons and nodes. Depending on how the network is trained, ANNs are divided into two categories: feedforward-propagation and back-propagation. Back-propagation ANNs are usually used in studies due to their better performance in various fields. One of the most common back-propagation ANNs is the multi-layer perceptron (MLP) network (Pradhan and Lee, 2010). Input data in MLP network will be connected to the hidden layer using a number of weights and biases in each neuron through an activation function. The activation (transformation) function is chosen depending on the performance. By using a set of training data these weights and biases will be determined and later be optimized through a number of iterations (Nedic et al., 2014).

In this study, we used a 7-layer MLP network with mean square error value as a validation criterion for network performance. The input features consisted of the main anomaly pixel corresponding to the earthquake, plus 3 pixels around it for the day before the earthquake using 1 km buffer around it, and also 5 pixels around the mentioned 3 pixels, making it 9 features altogether. Figure 2 shows the architecture of the MLP network.

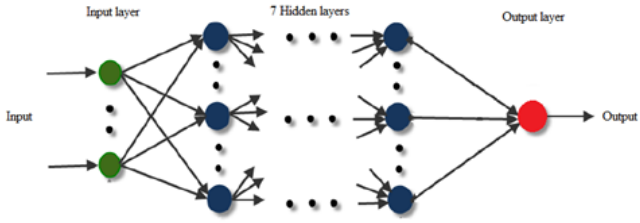

Figure 2: Architecture of the MLP network used in this study. It consists of 9 input features, 7 hidden layers, and the output layer.

Since each earthquake under investigation happened in a different region and time of the year, the base temperature is different in each case. The different temperature between the detected anomaly pixel and its surrounding pixels in various buffers and days are the input data for training this network so that the different temperatures in each region do not cause a problem. Also, all the temperature data used for training belongs to 30 days before the earthquake. In other words, the temperatures related to the 10 days after the earthquake in each case study are not used for training ANN.

4. RESULTS AND DISCUSSION

4.1. Land surface temperature diagram

As mentioned, for each earthquake, the LSTs for each buffer zone were categorized and by using the LST mean of each buffer, its 3D-diagram was created (Figure 3) and used as input data in thermal anomaly detection methods. Each pixel in these diagrams represents the LST mean (in Kelvin) in a certain radius buffer zone for a specific day. The red lines in Figure 3 show the day of the earthquake for each case.

Due to using the proposed method for grouping the LST data, some of the anomalies can be seen even visually around the time of the earthquake. Although relying only on visual aspects isn't accurate enough, it can be used for better presenting and understanding the situation.

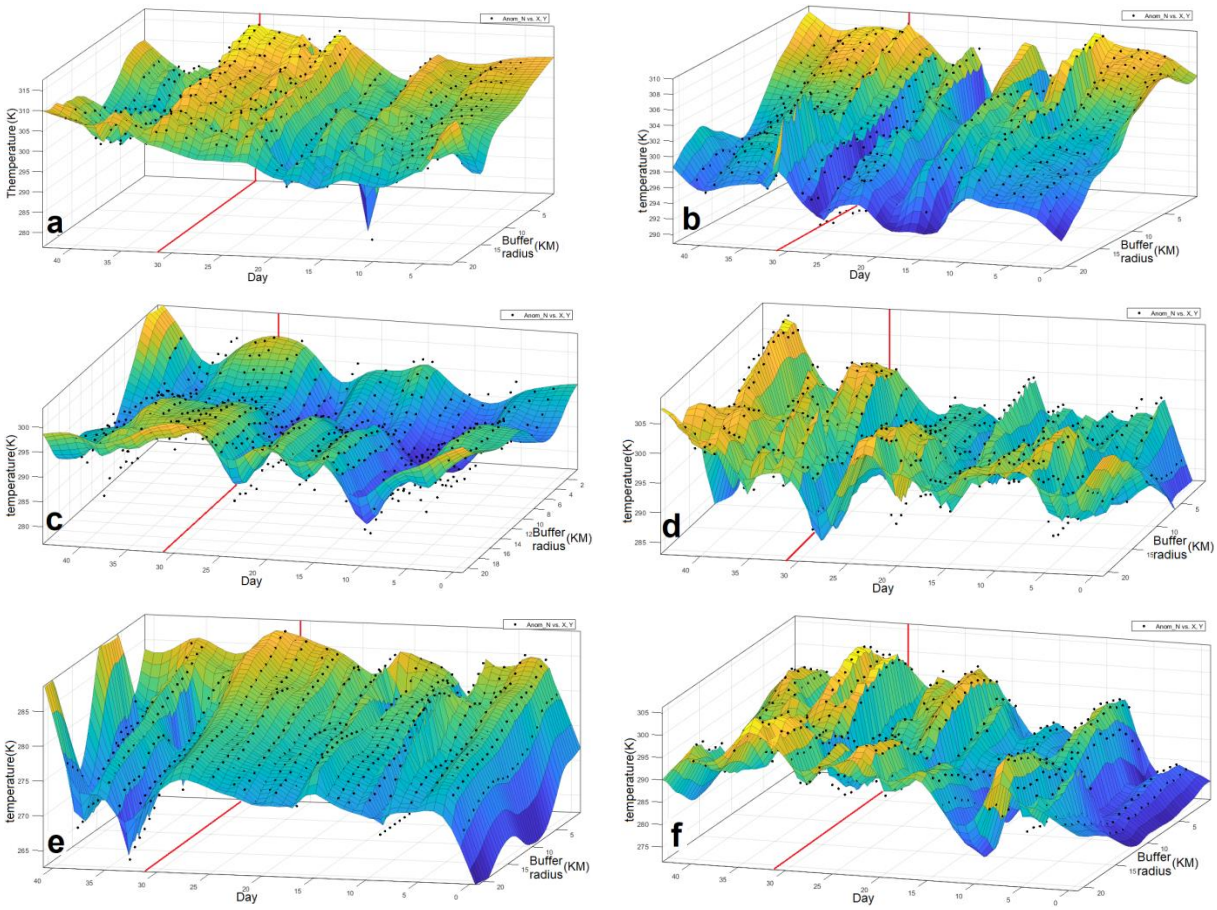

Figure 3: Land surface temperature diagram for a) Azgalah, b) Goharan, c) Saravan, d) Shonbeh, e) Brujerd, f) Sari case studies where in each case, the earthquake day is 31th day.

4.2. Detected thermal anomalies

In Figure 4 and Figure 5, the output of each anomaly detection method for each earthquake is shown. Results of each earthquake investigation show that the thermal anomaly is detectable in both of the anomaly detection methods mostly on the closest day to the earthquake regarding the closest buffer zone to the fault. These anomaly detection methods were used in other studies by using conventional selection of data as input. Although they have detected some anomalies, their accuracy was always in question due to many false alarm anomalies detected along with the actual anomaly.

Results show that in Azgalah, Goharan, Saravan, Brujerd, and Sari case studies, the anomalies detected by both methods are either on the day of the earthquake, the day before, the day after, or all of the days mentioned. This difference is due to the temporal proximity between the time of the imaging and the earthquake and the earthquake's intensity. In Shonbeh case study, although a thermal anomaly was detected on the day of the earthquake, another slightly stronger anomaly was detected 8 days after that.

It should be noted that the anomalies detected in far distance buffers from the corresponding fault are different for each earthquake (mostly in Saravan and Sari case studies) and do not have similar patterns. Moreover, since these pixels are far away from the corresponding fault and epicenter, it cannot be said for certain that they are related to the earthquake. Therefore, these pixels were not considered as earthquake-related anomalies and only anomalies in close distance buffers were used as earthquake-related anomalies in ANN algorithms.

The difficulty of this method is in far distances. For example, in buffers as far as 20 km radius from the fault, two pixels inside the buffer can be up to 80 km apart from each other, depending on the length of the fault itself. As a result, buffers with large radiuses could have pixels with various land covers and different temperatures. While limiting the buffer radius could shorten radiuses from the fault, it would make the area and diagram under investigation become too small, causing the method to be less effective.

Changing the coefficient value (k) for each anomaly detection process affects the result. The higher the value of coefficient k is, the higher the threshold for anomaly detection is set. This reduces the anomalies that can be detected while lowering the number of false alarm anomalies. On the other hand, increasing the coefficient value could result in omitting even the main anomaly that is related to the earthquake. Therefore, it is necessary to find an optimal value to increase the efficiency of each method. In this study, the coefficient value for the standard method is around 1.6 and for the interquartile method is around 1.3.

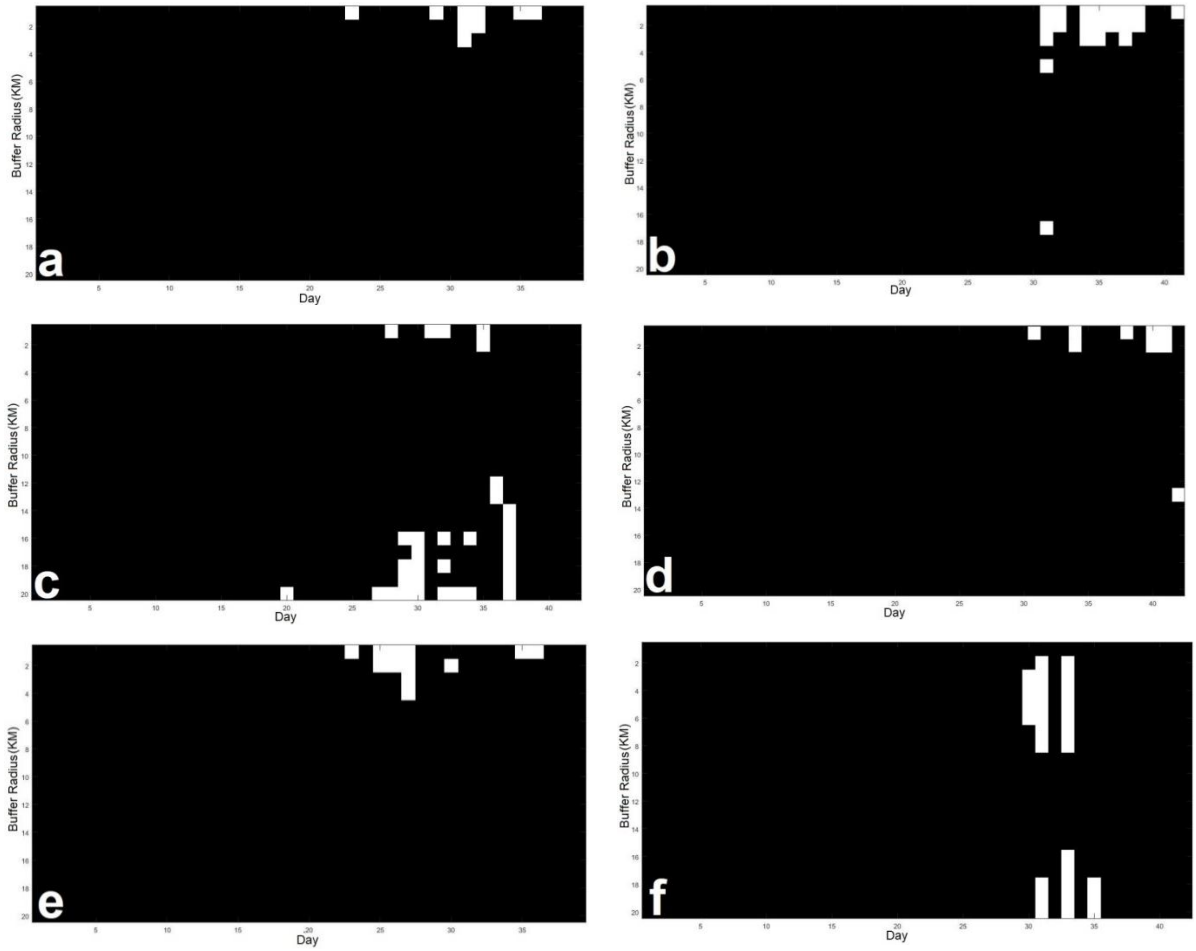

Figure 4: Simple anomaly detection method results for a) Azgalah, b) Goharan, c) Saravan, d) Shonbeh, e) Brujerd, f) Sari case studies where in each case, the earthquake day is 31th day.

4.3. The impact of difference in anomaly detection methods

The results show that both anomaly detection methods do find the thermal anomaly caused by seismic activities in each investigated earthquake. However, the interquartile anomaly detection method has a slightly more specified outcome and fewer false alarm anomalies.

Figure 4 shows the results for a standard anomaly detection method. It indicates the anomalies detected around the time of the earthquake in the nearest buffer from the corresponding fault. In Azgalah, Saravan, and Brujerd cases, few anomalies are detected before the earthquake while in Goharan and Shonbeh cases few anomalies are detected after the earthquake. In Sari case, the earthquake related anomalies are detected on the day of the earthquake. However, the anomaly is not detected in the nearest buffer but in the 2-8 km buffer zones. In Azgalah, Saravan, and Brujerd cases, some of the anomalies were detected around 6 days before the earthquake. Although these anomalies are not as strong as the anomalies detected near the time of the earthquake, they seem to be related to some seismic activities rather than being a false alarm.

Results for the interquartile anomaly detection method can be seen in Figure 5. Many anomalies detected by this method are related to the earthquake and found near the time of the earthquake in the closest buffer to the corresponding fault with the exception of Shonbah earthquake. As mentioned before, in Shonbah case study, another thermal anomaly was detected beside the main.

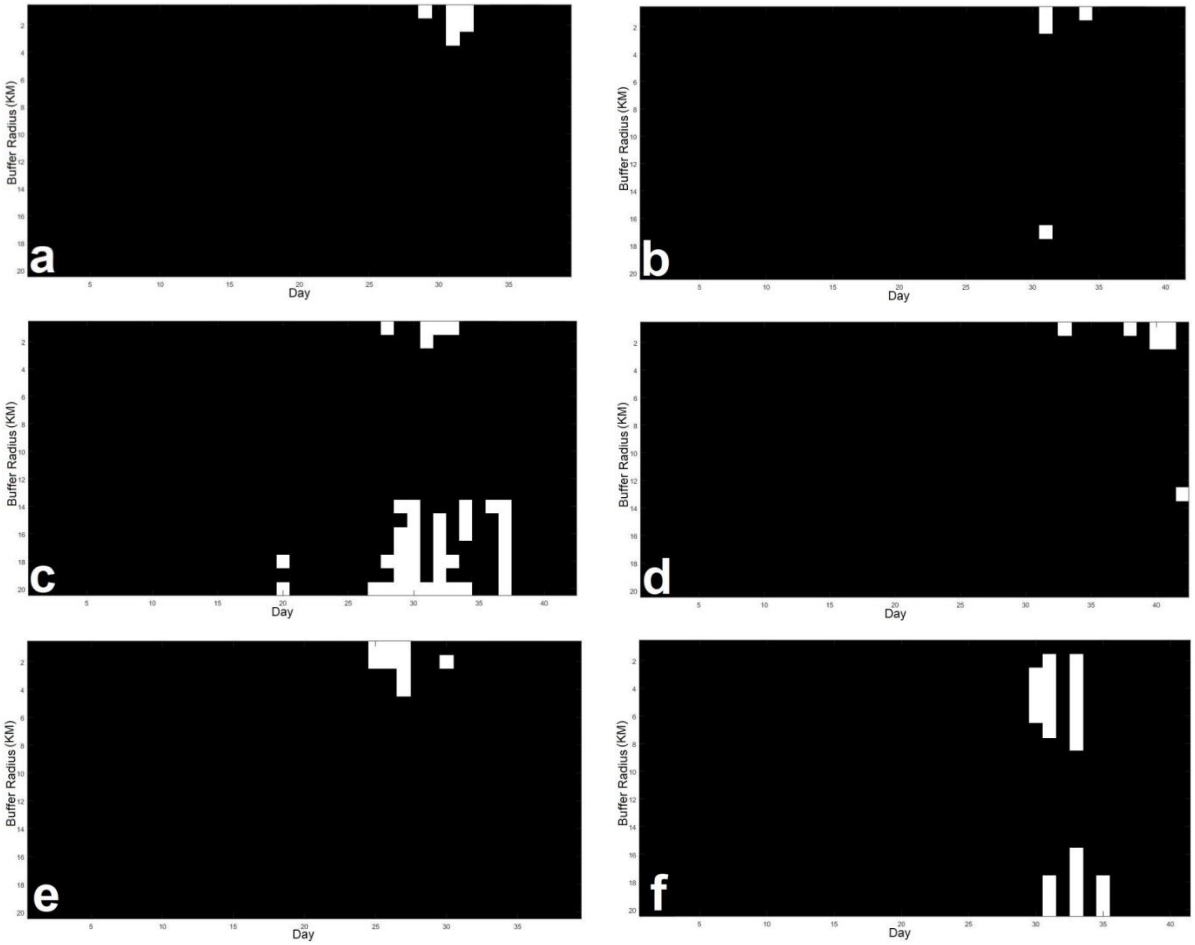

Figure 5: Interquartile anomaly detection method results for a) Azgalah, b) Goharan, c) Saravan, d) Shonbeh, e) Brujerd, f) Sari case studies where in each case, the earthquake day is 31th day

*Anomaly, almost **8** days after the earthquake, which was even stronger than the anomaly related to the earthquake. Nevertheless, these results show that the interquartile anomaly detection method has more specified results and a better outcome for training ANN, compared to the standard anomaly detection method.*

4.3. ***Artificial Neural Network (ANN) results***

Since interquartile method created more precise inputs for training the ANN, the anomalies detected by this method were used. Table 2 shows the results of each earthquake's estimated intensity and its accuracy compared to its actual intensity. The results indicate that the best accuracy belongs to Azgalah and the one with the least accuracy belongs to Sari case study. ANN results also show high correlation coefficients between thermal anomaly data and the earthquakes intensity.

It should be mentioned that a strong earthquake has greater anomaly at the earthquake point on the day of the earthquake and also in the nearest buffer to the fault.

Table 2. Estimated intensity for each earthquake using ANN

Earthquake	*Estimated Intensity*	*Error*	*Actual Intensity*
Azgalah	*7.301*	*0.001*	*7.3*
Goharan	*6.302*	*0.102*	*6.2*
Saravan	*7.719*	*0.081*	*7.8*
Shonbeh	*6.290*	*0.010*	*6.3*
Brujerd	*6.280*	*0.020*	*6.1*
Sari	*6.245*	*0.145*	*6.3*

Figure 6 shows the performance of the generated networks for each earthquake case based on mean square error (MSE).

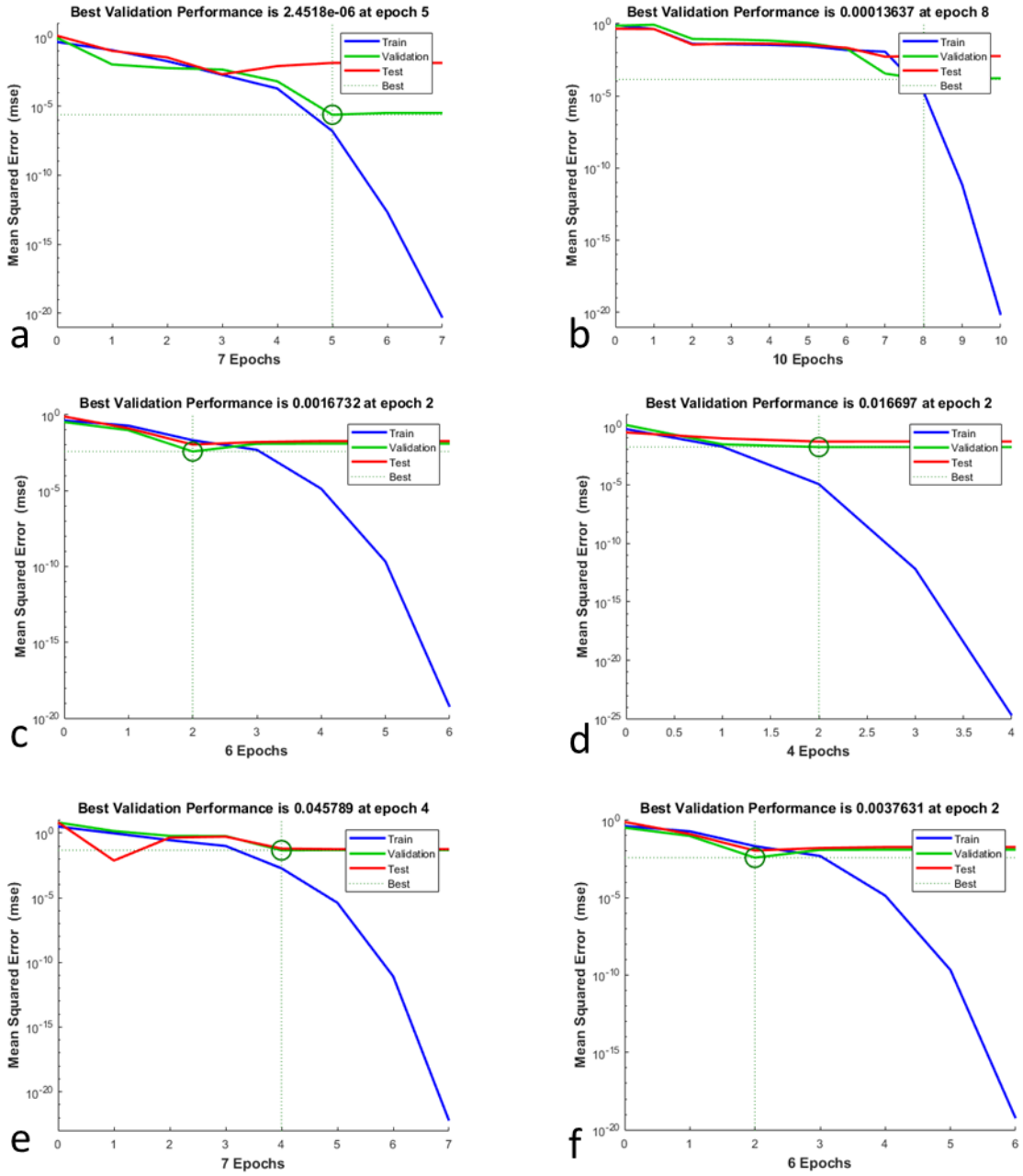

Figure 6 ANN performance base on mean squared error for a) Azgalah, b) Goharan, c) Saravan, d) Shonbeh, e) Brujerd, f) Sari case studies

*Regarding the limited number of investigated earthquakes, ANN presented a significant result by managing to sustain good accuracy using various thermal data for each earthquake. This figure shows at which epoch, network has its lowest MSE, or its variation is so insignificant that it is considered to be invariant in the next epochs. Figure **7** shows the correlation coefficient (R) between each network and the actual target value in each case study. As it can be seen the estimated intensities and the actual intensities for training and test data are very close for each case study. This fact allowed the generated network to have the value of correlation coefficient (R) above **0.98** between each network and its actual target value in each case study.*

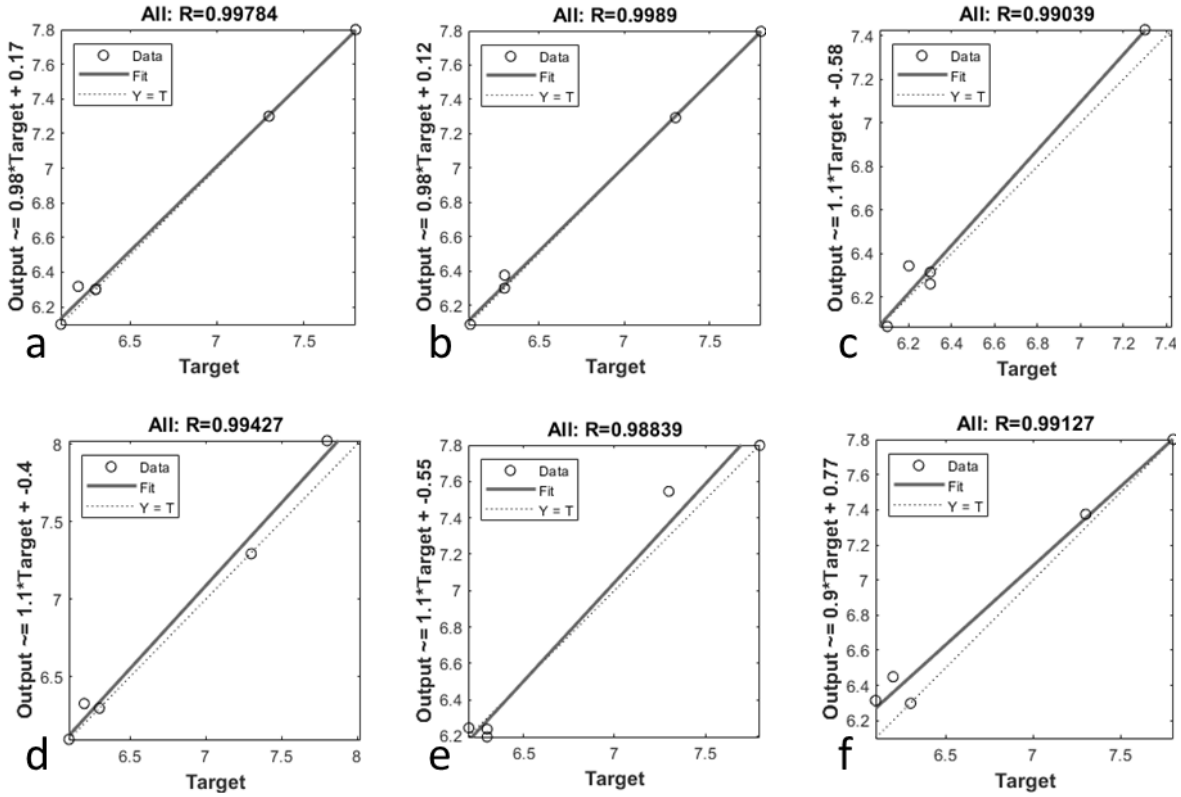

Figure 7 ANN's correlation coefficient (R) for a) Azgalah, b) Goharan, c) Saravan, d) Shonbeh, e) Brujerd, and f) Sari case studies.

5. CONCLUSION

Thermal anomaly is indeed a significant precursor for strong earthquakes. The proposed method which includes analyzing the anomalies with respect to the buffer zones in different distances relevant to faults, increases the accuracy dramatically. Two thermal anomaly detection methods were used for investigating each earthquake in this study. Although the outcome of each method is slightly different from another for each earthquake, the interquartile method has better results compared to the standard method. Nevertheless, they are both more accurate when anomaly detection algorithms use the proposed grouped input data instead of the ordinary selection of data.

ANN results show that thermal anomaly data highly corresponds with earthquake intensity. Thus, the network was constructed properly, making the estimated results close to actual intensities. It is recommended to use more data related to more earthquakes and different locations for training ANN to improve the network accuracy.

However, it should be pointed out that thermal anomaly on its own is not quite sufficient for estimating earthquake parameters and activities. It is highly recommended to use it as an initial and primary precursor for limiting the search area and then use other precursors, which require more complicated data and methods. Thermal anomaly precursors can also be used in combination with other simple precursors to get efficient and comprehensive results.

Many previous studies that investigated thermal anomalies, explored areas only around the epicenter. Methods used in such studies required the exact location of epicenter therefore they are only possible after happening of the earthquake. Since the location of the active faults is known a priori or can be identified by further investigations, using the fault distance-based approach can be a superior method in predicting the impending earthquakes for vulnerable faults. In spite of the previous investigations that the studies were only possible aftermath, the fault distance-based approach can be used as a tool for impending unknown earthquake prediction.

References

Adeli, H. (1999). Machine Learning - Neural Networks, Genetic Algorithms and Fuzzy Systems. Kybernetes.

Akhoondzadeh, M. (2012). Anomalous TEC variations associated with the powerful Tohoku earthquake of 11 March 2011. Natural Hazards and Earth System Sciences, 12(5), 1453.

Akhoondzadeh, M. (2014). Thermal and TEC anomalies detection using an intelligent hybrid system around the time of the Saravan, Iran,(Mw= 7.7) earthquake of 16 April 2013. Advances in Space Research, 53(4), 647-655.

Cheng, J., & Li, Q. (2008). Reliability analysis of structures using artificial neural network based genetic algorithms. Computer methods in applied mechanics and engineering, 197(45-48), 3742-3750.

Choudhury, S., Dasgupta, S., Saraf, A. K., & Panda, S. (2006). Remote sensing observations of pre-earthquake thermal anomalies in Iran. International Journal of Remote Sensing, 27(20), 4381-4396.

Chung, S.-H., Lee, A. H., & Pearn, W.-L. (2005). Analytic network process (ANP) approach for product mix planning in semiconductor fabricator. International journal of production economics, 96(1), 15-36.

Cicerone, R. D., Ebel, J. E., & Britton, J. (2009). A systematic compilation of earthquake precursors. Tectonophysics, 476(3-4), 371-396.

Console, R., Pantosti, D., & D'Addezio, G. (2002). Probabilistic approach to earthquake prediction. Annals of geophysics, 45(6).

Ergu, D., Kou, G., Shi, Y., & Shi, Y. (2014). Analytic network process in risk assessment and decision analysis. Computers & Operations Research, 42, 58-74.

Freund, F. (2011). Pre-earthquake signals: Underlying physical processes. Journal of Asian Earth Sciences, 41(4-5), 383-400.

Geller, R. J., Jackson, D. D., Kagan, Y. Y., & Mulargia, F. (1997). Earthquakes cannot be predicted. Science, 275(5306), 1616-1616.

Hayakawa, M., Molchanov, O., Kodama, T., Tanaka, T., & Igarashi, T. (2000). On a possibility to monitor seismic activity using satellites. Advances in Space Research, 26(6), 993-996.

Khalili, M., Abdollahi Eskandar, S. S., & Alavi Panah, S. K. (2020). Thermal anomalies detection before Saravan earthquake (April 16th, 2013, MW= 7.8) using time series method, satellite, and meteorological data. Journal of Earth System Science, 129, 1-10.

Li, B., Shi, Z., Wang, G., & Liu, C. (2019). Earthquake-related hydrochemical changes in thermal springs in the Xianshuihe Fault zone, Western China. Journal of hydrology, 579, 124175.

Nedic, V., Despotovic, D., Cvetanovic, S., Despotovic, M., & Babic, S. (2014). Comparison of classical statistical methods and artificial neural network in traffic noise prediction. Environmental Impact Assessment Review, 49, 24-30.

Nekoee, M., & Shah-Hosseini, R. (2020). Thermal anomaly detection using NARX neural network method to estimate the earthquake occurrence time. Earth Observation and Geomatics Engineering, 4(2), 98-108.

Ouzounov, D., & Freund, F. (2004). Mid-infrared emission prior to strong earthquakes analyzed by remote sensing data. Advances in Space Research, 33(3), 268-273.

Pradhan, B., & Lee, S. (2009). Landslide risk analysis using artificial neural network model focusing on different training sites. Int J Phys Sci, 3(11), 1-15.

Pradhan, B., & Lee, S. (2010). Delineation of landslide hazard areas on Penang Island, Malaysia, by using frequency ratio, logistic regression, and artificial neural network models. Environmental Earth Sciences, 60(5), 1037-1054.

Qiang, Z.-j., Xu, X.-d., & Dian, C.-g. (1997). Case 27 thermal infrared anomaly precursor of impending earthquakes. Pure and Applied Geophysics, 149(1), 159-171.

Qiang, Z., Dian, C., Li, L., Xu, M., Ge, F., Liu, T., . . . Guo, M. (1999). Atellitic thermal infrared brightness temperature anomaly image—short-term and impending earthquake precursors. Science in China series D: Earth Sciences, 42(3), 313-324.

Rawat, V., Saraf, A. K., Das, J., Sharma, K., & Shujat, Y. (2011). Anomalous land surface temperature and outgoing long-wave radiation observations prior to earthquakes in India and Romania. Natural hazards, 59(1), 33-46.

Roeloffs, E. A. (1988). Hydrologic precursors to earthquakes: A review. Pure and Applied Geophysics, 126, 177-209.

Sahoo, S., Dhar, A., & Kar, A. (2016). Environmental vulnerability assessment using Grey Analytic Hierarchy Process based model. Environmental Impact Assessment Review, 56, 145-154.

Saradjian, M., & Akhoondzadeh, M. (2011). Thermal anomalies detection before strong earthquakes (M> 6.0) using interquartile, wavelet and Kalman filter methods. Natural Hazards and Earth System Sciences, 11(4), 1099.

Saraf, A., & Choudhury, S. (2005). Cover: satellite detects surface thermal anomalies associated with the Algerian earthquakes of May 2003. International Journal of Remote Sensing, 26(13), 2705-2713.

Saraf, A. K., Rawat, V., Choudhury, S., Dasgupta, S., & Das, J. (2009). Advances in understanding of the mechanism for generation of earthquake thermal precursors detected by satellites. International Journal of Applied Earth Observation and Geoinformation, 11(6), 373-379.

Surkov, V., Pokhotelov, O., Parrot, M., & Hayakawa, M. (2006). On the origin of stable IR anomalies detected by satellites above seismo-active regions. Physics and Chemistry of the Earth, Parts A/B/C, 31(4-9), 164-171.

Tramutoli, V. (1998). Robust AVHRR Techniques (RAT) for environmental monitoring: theory and applications. Paper presented at the Earth surface remote sensing II.

Tramutoli, V., Cuomo, V., Filizzola, C., Pergola, N., & Pietrapertosa, C. (2005). Assessing the potential of thermal infrared satellite surveys for monitoring seismically active areas: The case of Kocaeli (Izmit) earthquake, August 17, 1999. Remote Sensing of Environment, 96(3-4), 409-426.

Tramutoli, V., Di Bello, G., Pergola, N., & Piscitelli, S. (2001). Robust satellite techniques for remote sensing of seismically active areas.

Tronin, A. (1996). Satellite thermal survey—a new tool for the study of seismoactive regions. International Journal of Remote Sensing, 17(8), 1439-1455.

Verma, M., & Bansal, B. K. (2012). Earthquake precursory studies in India: Scenario and future perspectives. Journal of Asian Earth Sciences, 54, 1-8.

Wang, C.-y., & Manga, M. (2021). Earthquakes influenced by water. In Water and Earthquakes (pp. 61-82): Springer.

Wyss, M. (1997). Cannot earthquakes be predicted? Science, 278(5337), 487-490.

Yao, Q. (2007). Field effect and regional conversion as the mechanism of natural hazard chains. Meteorol Disaster Reduct Res, 30(3), 31-36.